

## Supporting Information

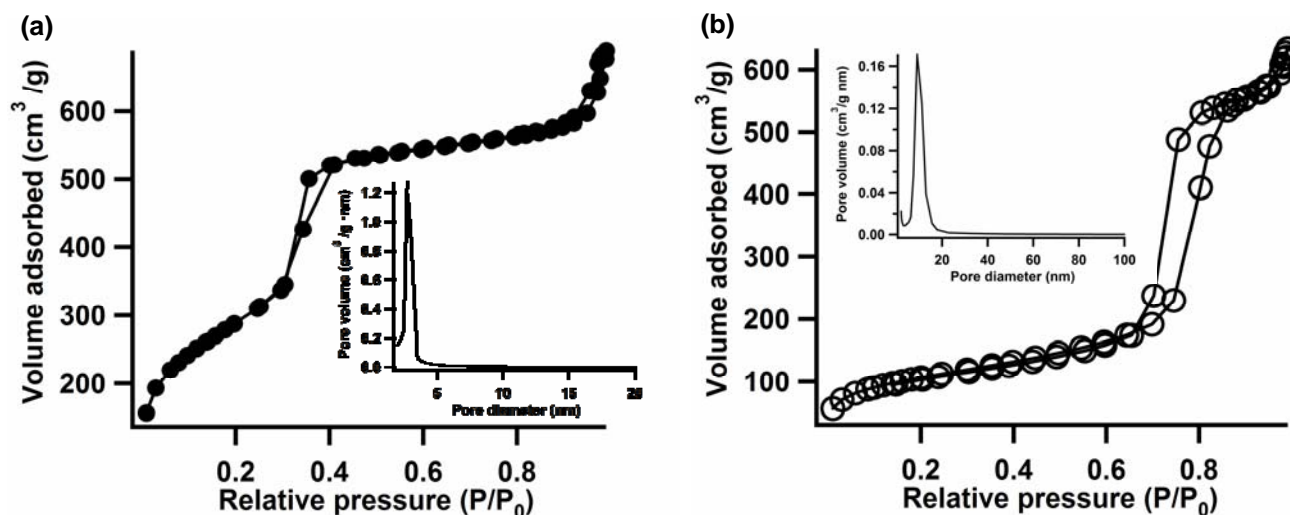
### Interaction of Mesoporous Silica Nanoparticles with Human Red Blood

#### Cell Membranes: Size and Surface Effects

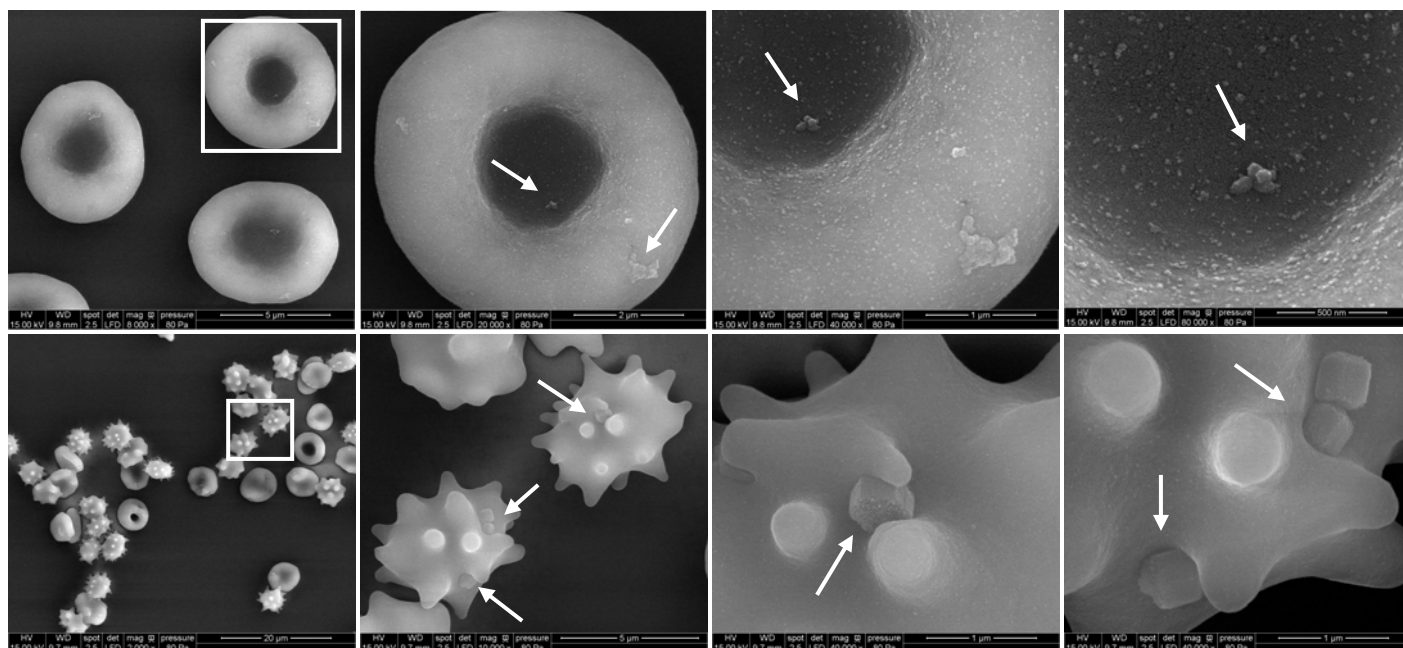
Yannan Zhao, Xiaoxing Sun, Guannan Zhang, Brian G. Trewyn\*, Igor I. Slowing\*, and Victor S.-Y. Lin

Department of Chemistry, U.S. Department of Energy Ames Laboratory, Iowa State University, Ames,  
Iowa 50011-3111, U.S.A.

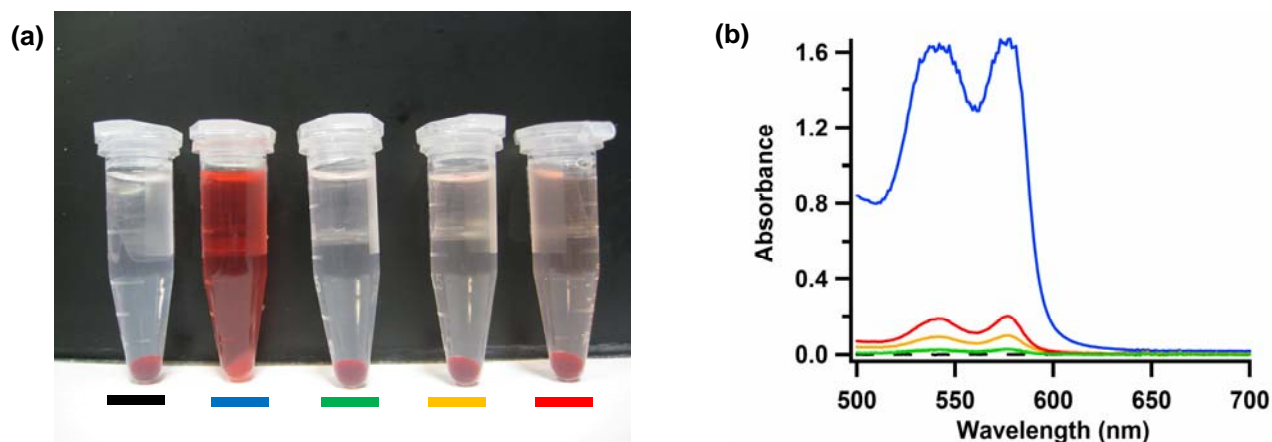
\*Address correspondence to: bgrewyn@iastate.edu and islowing@iastate.edu



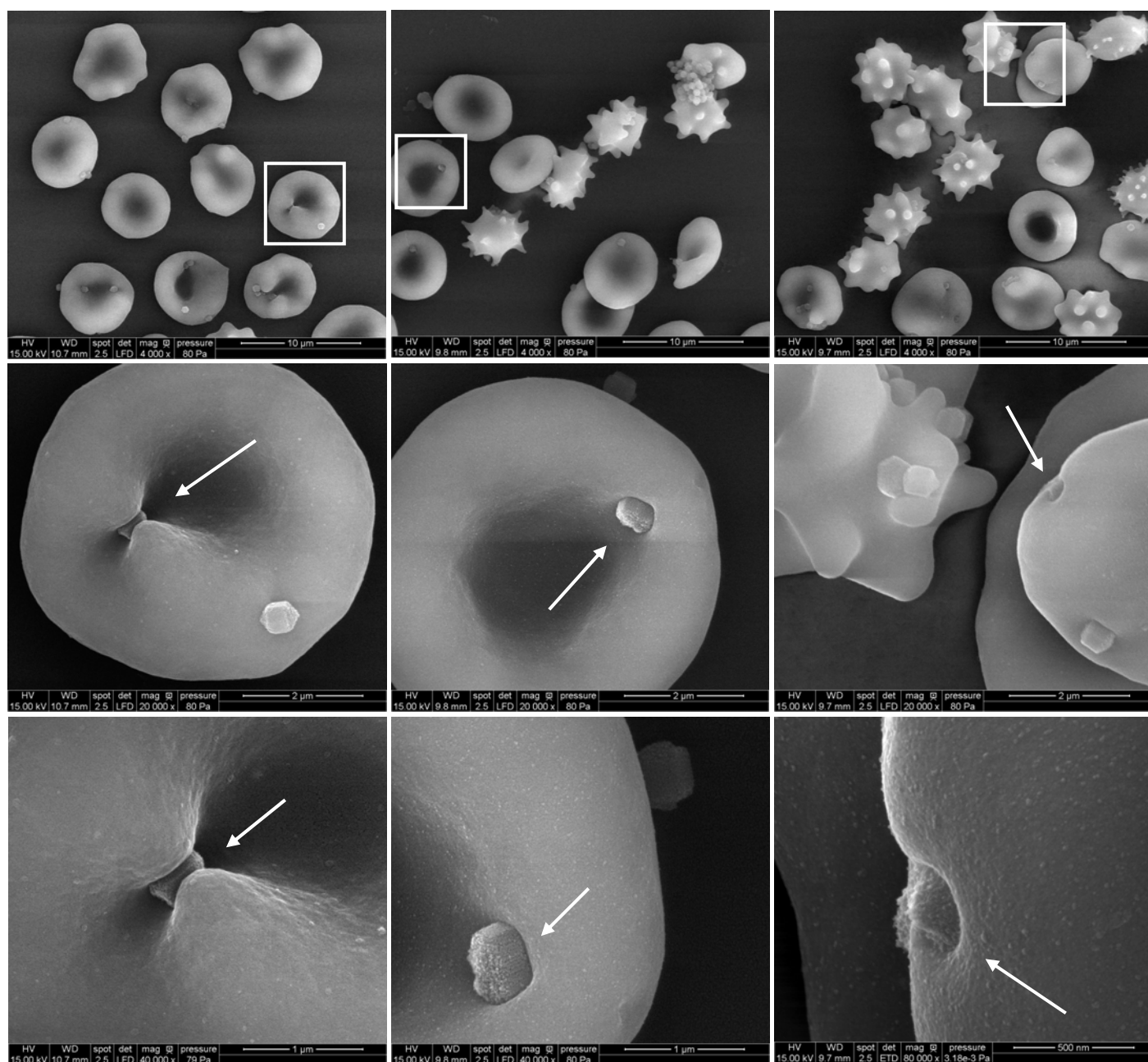
**Figure S1.** Linear plot of the nitrogen sorption isotherms and pore size distributions of (a) *s*-MSN and (b) *l*-MSN. Surface areas of *s*-MSN and *l*-MSN were calculated to be  $1051.6 \pm 2.2 \text{ m}^2 \text{ g}^{-1}$  and  $387.0 \pm 1.3 \text{ m}^2 \text{ g}^{-1}$ , respectively.



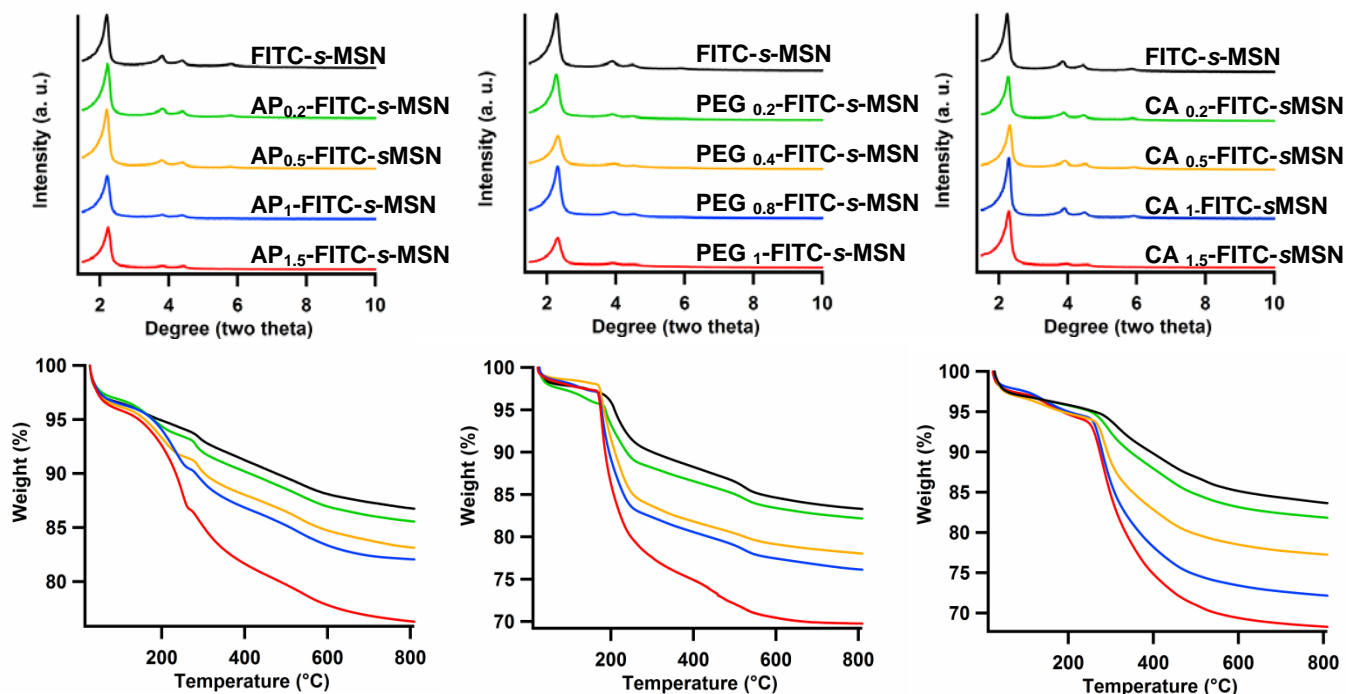
**Figure S2.** Scanning electron micrographs (SEM) of RBCs (5% hematocrit) incubated with  $100 \mu\text{g mL}^{-1}$  *s*-MSN (top) and *l*-MSN (bottom). Images increase in magnification from left to right with features highlighted with white squares or arrows, indicating the location of particles attached on RBC membrane.



**Figure S3.** Hemolysis assay for *l*-MSN using water as a positive control (blue lines) and PBS as a negative control (dashed black lines). The materials were suspended at 20 (green), 50 (yellow) and 100 (red)  $\mu\text{g mL}^{-1}$ . The mixtures were centrifuged to detect the presence of hemoglobin (red) in the supernatant visually (a) and by absorption at 541 nm (b).



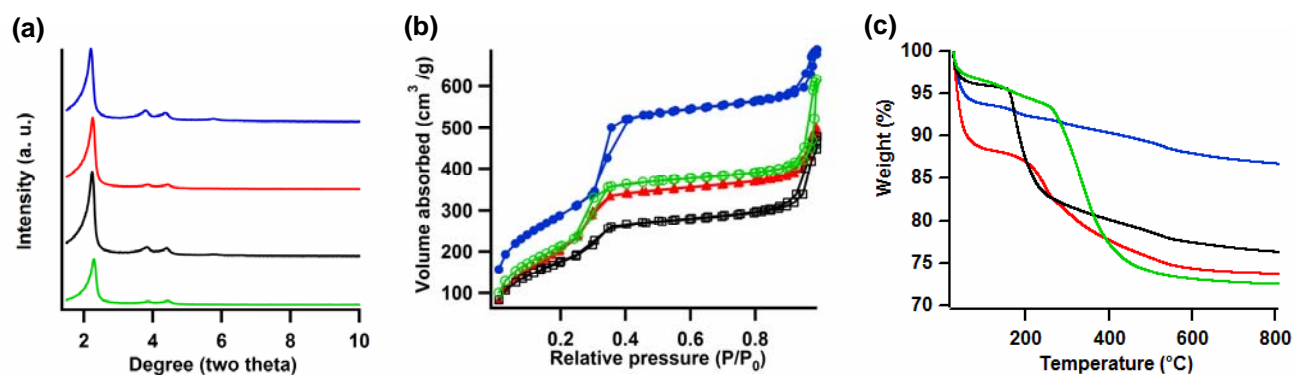
**Figure S4.** Scanning electron micrographs (SEM) of RBCs (5% hematocrit) incubated with 20  $\mu\text{g mL}^{-1}$  (left), 50  $\mu\text{g mL}^{-1}$  (middle), and 100  $\mu\text{g mL}^{-1}$  of *l*-MSN (right). Percent of spiculated RBCs were observed to be < 10%, ~50% and ~90% from left to right. Images increase in magnification from top to bottom with features highlighted with white squares or arrows, indicating the location of particles attached on RBC membrane.



**Figure S5.** X-ray diffraction patterns (top) and thermogravimetric analysis (bottom) of FITC-*s*-MSN, AP<sub>*x*</sub>-FITC-*s*-MSN (left), PEG<sub>*x*</sub>-FITC-*s*-MSN (middle) and CA<sub>*x*</sub>-FITC-*s*-MSN (right) (*x*: amount of organic groups introduced in mmol g<sup>-1</sup>).

**Table S1.** Characteristics of FITC-*s*-MSN, AP<sub>*x*</sub>-FITC-*s*-MSN, PEG<sub>*x*</sub>-FITC-*s*-MSN and CA<sub>*x*</sub>-FITC-*s*-MSN (*x*: amount of organic groups introduced in mmol g<sup>-1</sup>).

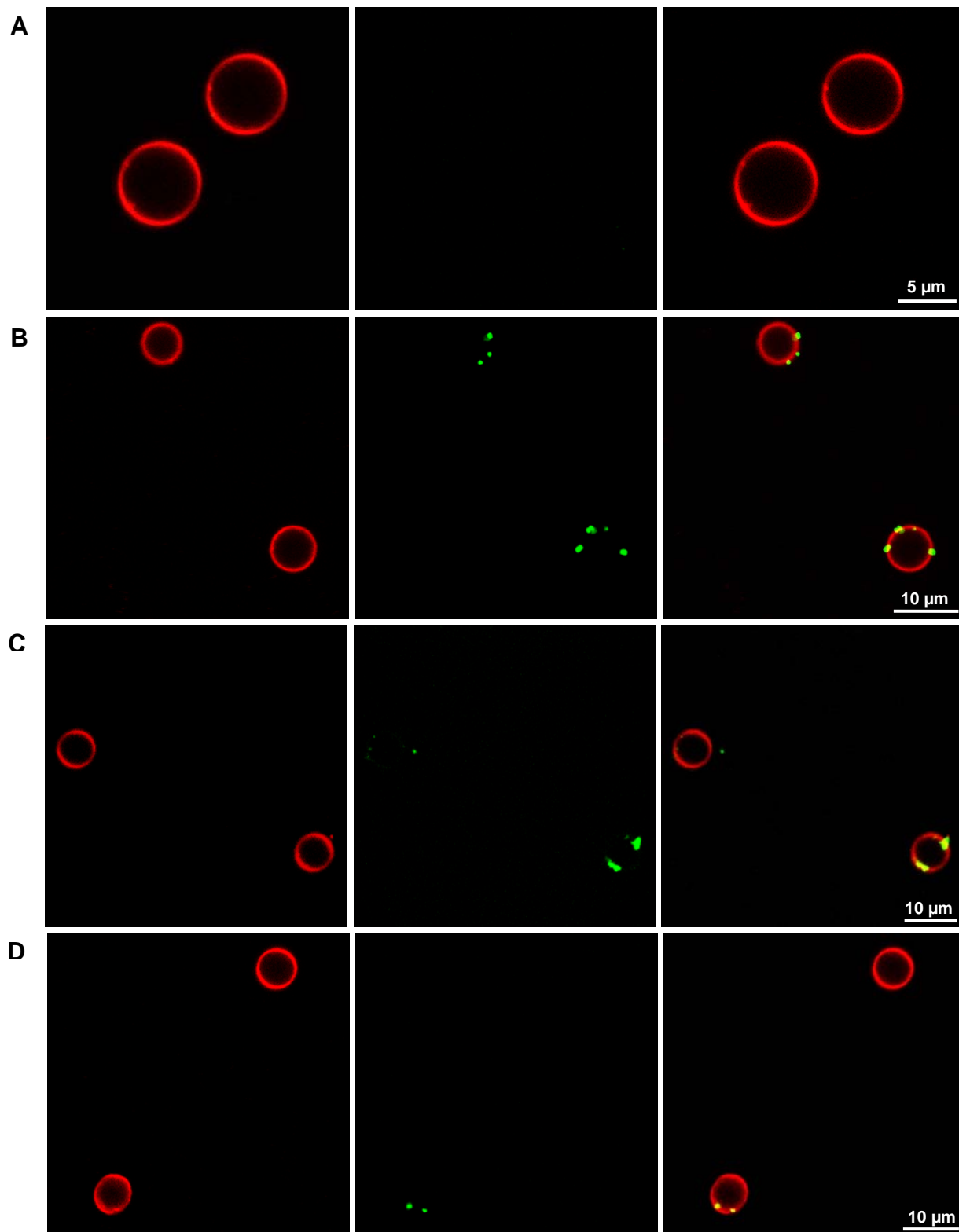
Materials	Surface groups (mmol g <sup>-1</sup> )	Zeta potential (mV)	Surface area (m <sup>2</sup> g <sup>-1</sup> )	Pore size (nm)
FITC- <i>s</i> -MSN	0.02	-27.9	1043.4 ± 4.2	3.0
AP <sub>0.2</sub> -FITC- <i>s</i> -MSN	0.1-0.2	-22.9	948.3 ± 7.9	2.8
AP <sub>0.5</sub> -FITC- <i>s</i> -MSN	0.4-0.6	-10.9	878.7 ± 11.7	2.8
AP <sub>1</sub> -FITC- <i>s</i> -MSN	0.6-0.8	+3.2	796.8 ± 1.6	2.8
AP <sub>1.5</sub> -FITC- <i>s</i> -MSN	1.2-1.6	+6.87	689.0 ± 29.0	2.7
FITC- <i>s</i> -MSN	0.03	-29.3	1036.4 ± 11.2	2.6
PEG <sub>0.2</sub> -FITC- <i>s</i> -MSN	0.03-0.04	-26.1	985.6 ± 9.0	2.6
PEG <sub>0.4</sub> -FITC- <i>s</i> -MSN	0.1-0.2	-22.3	839.6 ± 9.3	2.4
PEG <sub>0.8</sub> -FITC- <i>s</i> -MSN	0.2-0.3	-20.7	770.8 ± 1.6	2.4
PEG <sub>1</sub> -FITC- <i>s</i> -MSN	0.4-0.5	-13.1	628.9 ± 2.6	2.4
FITC- <i>s</i> -MSN	0.03	-28.6	1107.8 ± 8.6	2.7
CA <sub>0.2</sub> -FITC- <i>s</i> -MSN	0.07-0.1	-34.3	967.4 ± 2.9	2.5
CA <sub>0.5</sub> -FITC- <i>s</i> -MSN	0.3-0.4	-36.1	913.6 ± 19.2	2.4
CA <sub>1</sub> -FITC- <i>s</i> -MSN	0.5-0.7	-39.2	863.0 ± 9.2	2.4
CA <sub>1.5</sub> -FITC- <i>s</i> -MSN	0.7-1	-42.7	779.2 ± 5.0	2.5



**Figure S6.** (a) X-ray diffraction (XRD) patterns, (b) linear plot of the nitrogen sorption isotherms and (c) thermogravimetric analysis (TGA) of *s*-MSN (blue), AP<sub>1.5</sub>-*s*-MSN (red), PEG<sub>1</sub>-*s*-MSN (black) and CA<sub>1.5</sub>-*s*-MSN (green).

**Table S2.** Characteristics of *s*-MSN, AP<sub>1.5</sub>-*s*-MSN, PEG<sub>1</sub>-*s*-MSN, CA<sub>1.5</sub>-*s*-MSN and *l*-MSN.

Materials	Surface groups (mmol g <sup>-1</sup> )	Zeta potential (mV)	Surface area (m <sup>2</sup> g <sup>-1</sup> )	Pore size (nm)	Hydrodynamic particle size (nm)
<i>s</i> -MSN		-22.2	1051.6 ± 2.2	3.1	122
AP <sub>1.5</sub> - <i>s</i> -MSN	1.1-1.5	+5.79	780.3 ± 9.0	2.4	142
PEG <sub>1</sub> - <i>s</i> -MSN	0.3-0.4	-11.6	650.5 ± 2.9	2.7	122
CA <sub>1.5</sub> - <i>s</i> -MSN	0.6-0.9	-43.1	792.9 ± 4.4	2.9	142
<i>l</i> -MSN		-16.5	387.0 ± 1.3	9.0	531



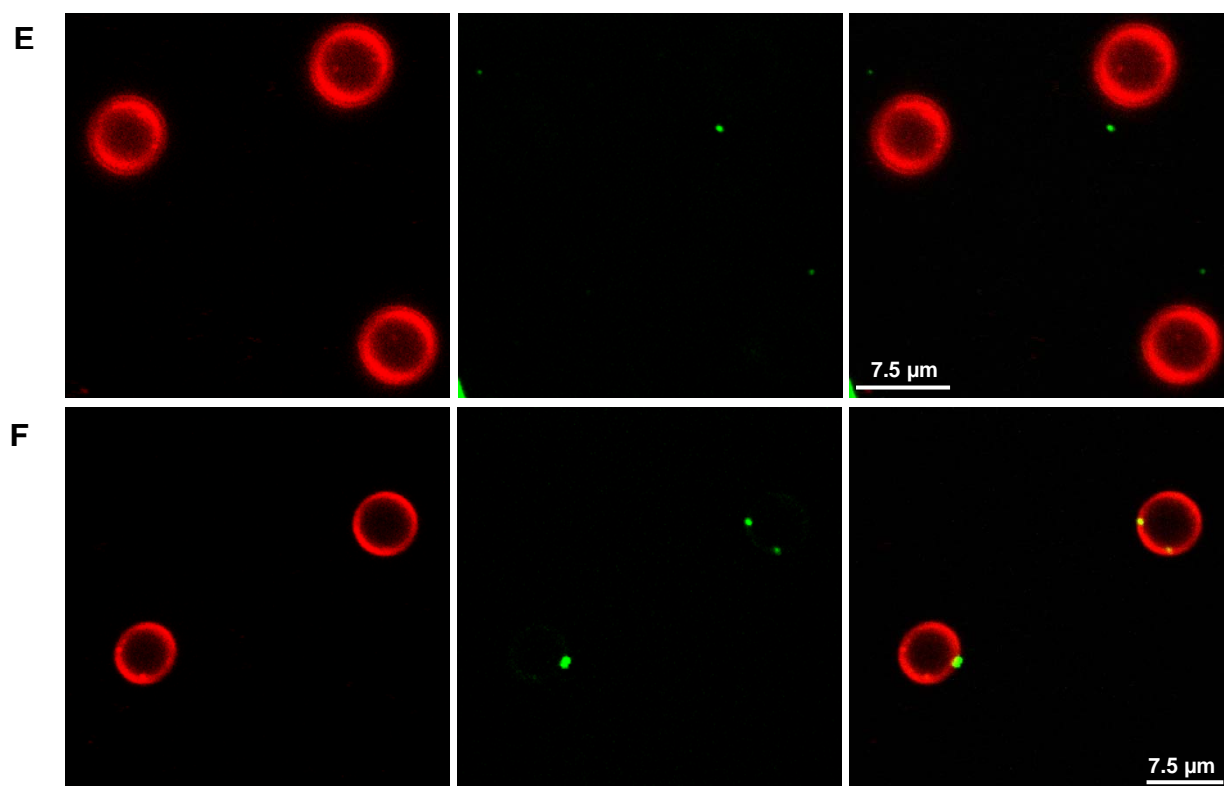


**Figure S7.** Confocal fluorescence micrographs of (A) RBCs ( $5 \times 10^6$  cells  $\text{mL}^{-1}$ ) incubated with  $20 \mu\text{g mL}^{-1}$  of (B) FITC-*l*-MSN, (C) FITC-*s*-MSN, (D) AP<sub>1.5</sub>-FITC-*s*-MSN, (E) PEG<sub>1</sub>-FITC-*s*-MSN and (F) CA<sub>1.5</sub>-FITC-*s*-MSN. The channels from left to right correspond to red blood cells stained with PKH26 red fluorescence dye, FITC-MSNs and the merged images.

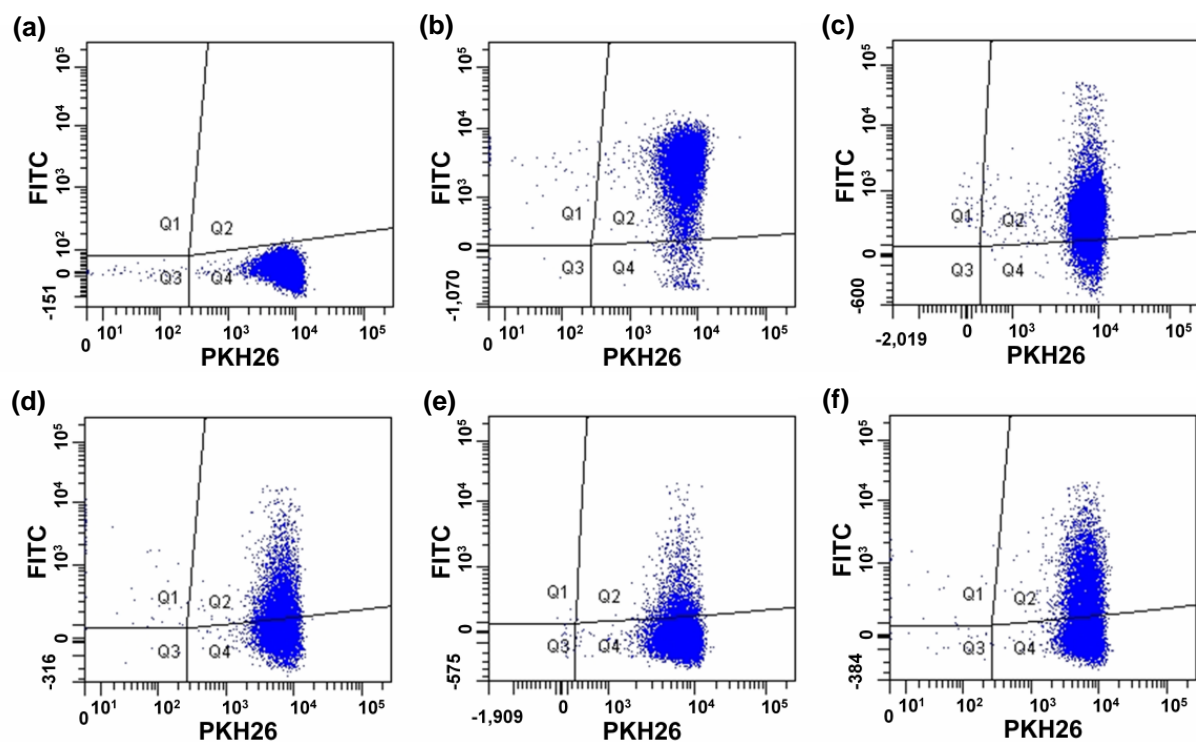


**Figure S8.** Dot plot from the flow cytometry analysis of (a) PKH26 labeled RBC incubated with (b) FITC-*l*-MSN, (c) FITC-*s*-MSN, (d) AP<sub>1.5</sub>-FITC-*s*-MSN, (e) PEG<sub>1</sub>-FITC-*s*-MSN and (f) CA<sub>1.5</sub>-FITC-*s*-MSN. The axes correspond to the intensity of red fluorescence due to PKH26 labeling (horizontal axis) and green fluorescence due to the attachment of FITC-MSNs onto PKH26-RBCs (vertical axis). The plot was gated to show PKH26 labeled RBCs in area Q4 and FITC-fluorescent PKH26-RBCs in area Q2.